Research Square

Preprints are preliminary reports that have not undergone peer review.
They should not be considered conclusive, used to inform clinical practice,
or referenced by the media as validated information.

Ziyuglycoside I attenuates collagen-induced arthritis through restoring the balance of Th17/Treg cells

Manman Wang
Anhui Medical University
Hanfei Sun
Anhui Medical University
Tiantian Su
Anhui Medical University
Paipai Guo
Anhui Medical University
Yu Tai
Anhui Medical University
Zhenduo Zhu
Anhui Medical University
Huijuan Cheng
Anhui Medical University
Chunru Jiang
Anhui Medical University
Wei Wei
Anhui Medical University
Qingtong Wang (hfwqt727@163.com)
Anhui Medical University

Research Article

Keywords: rheumatoid arthritis, Th17/Treg, Ziyuglycoside I, mTOR, RORγt, Foxp3

Posted Date: March 31st, 2022

DOI: https://doi.org/10.21203/rs.3.rs-1462289/v1

License: This work is licensed under a Creative Commons Attribution 4.0 International License. Read Full License

Abstract

Objective: To investigate the therapeutic effect and primary pharmacological mechanism of Ziyuglycoside I (Ziyu I) on collagen-induced arthritis (CIA) mice.

Methods: CIA mice were treated by 5, 10, or 20 mg/kg of Ziyu I or 2 mg/kg of methotrexate (MTX), and clinical manifestations as well as pathological changes were observed. T cell subsets were determined by flow cytometry. T cell viability was measured by CCK-8. The expressions of transforming growth factor beta (TGF-β) and IL-17 in serum were detected by Elisa. The mRNA expressions of RORγt and Foxp3 in mice spleen lymphocytes were detected by RT-qPCR. Molecular docking was used to detect whether there was a molecular interaction between Ziyu I and Akt. The activation of mTOR in T cells was verified by Western blotting or immunofluorescence.

Results: Ziyu I treatment group could effectively alleviate the arthritis symptoms of CIA mice, including body weight, global score, arthritis index, number of swollen joints, etc. The pathological changes of joints and spleen in arthritic mice were improved effectively. The thymic index, T cell activity and RORγt production of Ziyu I treatment group were significantly reduced. Notably, through molecular docking, western blotting, and immunofluorescence analysis data, we found that Ziyu I could interact directly with Akt to reduce downstream mTOR activation and inhibit Th17 differentiation, thereby regulating Th17/Treg balance and improving arthritis symptoms.

Conclusion: Our data showed that Ziyu I effectively improved arthritic symptoms of CIA in mice by inhibiting mTOR activation, thereby affecting Th17 differentiation and regulating Th17/Treg balance.

1. Introduction

Rheumatoid arthritis (RA) is a systemic autoimmune disease that mainly characterized by chronic inflammation targeting synovial membrane, following with cartilage and bone erosion [1]. Although the precise pathogenesis of RA is unclear, both T cell and B cell activation are involved in the pathogenesis of RA [2]. Due to the continuous infiltration and activation of lymphocytes, joint synovial tissue suffers from abnormal proliferation, causing joint deformities and dysfunction. Th17 and Treg cells are formed by the activation of initial $CD4^+$ T cells stimulated by foreign antigens. It has been demonstrated that an imbalance in Th17/Treg cells had an important role in joint inflammation and destruction [3].

At present, we all know that most of the anti-rheumatic diseases have serious adverse drug reactions, so the development of safe and effective new anti-rheumatic diseases drugs is one of the hot spots of current pharmaceutical research. A large number of studies have shown that natural drugs have a significant immunomodulatory effect in the prevention and treatment of RA and have the unique advantages of less toxic side effects and less drug resistance [4, 5]. Glycosides and alkaloids such as total glucosides of paeony (TGP), total glucosides of panax ginseng are the main components of natural herbs with anti-inflammatory effects, and more effective and safer natural medicines are also being studied. Ziyuglycoside has been established as an herbal plant with medicinal use for a long time. Ziyuglycoside is rich in chemical components, mainly containing phenols, flavonoids, triterpenoids and other compounds. Ziyuglycoside I (Ziyu I) and Ziyuglycoside II in Ziyuglycoside have good anti-inflammatory and anticancer effects [6]. According to preliminary reports, Ziyu I exhibits a diverse array of promising properties, such as anti-inflammatory [7-9], antiedematous, anti-tumor, antimutagenic, venotonic, expectorant and broncholytic activities [10, 11]. However, whether Ziyu I has anti-rheumatism effect has not been studied.

In this study, we treated collagen-induced arthritis (CIA) mice with 3 different doses of Ziyu I or positive control drug methotrexate (MTX) for 4 weeks and observed an improvement in joint inflammation and a down-regulation of Th17 cell ratio after Ziyu I treatment. Our study suggests that Ziyu I may be a promising anti-rheumatoid arthritis drug.

2. Materials And Methods

2.1. Induction and treatment of collagen-induced arthritis in mice

Male DBA/1 mice (8-10 weeks old) were purchased from Shanghai SLAC Laboratory Animal Co., Ltd, and were housed in specific pathogen free laboratory of Institute of Clinical Pharmacology, Anhui Medical University with a 12 light/12 dark cycle. All protocols of these experiments have been approved by the Ethics Committee of Institute of Clinical Pharmacology, Anhui Medical University (Approval ID: PZ-2020-045). After a week of adaptive feeding, the mice were injected subcutaneously with 0.1 ml of chick type II collagen (CCII) emulsion (2 mg/ml immunization grade CCII (Catalog #:20011, Chondrex, Inc. Woodinville, WA, USA) dissolved in 0.05M acetic acid was emulsified with equal volume of Complete Freund's Adjuvant (CFA) containing 2 mg/ml heat-killed M. Tuberculosis H37 RA (Catalog #:7009, Chondrex, Inc. Woodinville, WA, USA) at the base of tail on day 0. Then on day 21, the same dose of CCII emulsion was subcutaneously injected into the tail or back of the mice to enhance immunity [12].

95% of mice injected with CCII emulsion successfully developed arthritis, then CIA mice were randomly divided into vehicle treatment; 5 mg/kg, 10 mg/kg, or 20 mg/kg of Ziyu I (Catalog #: B20294, HPLC≥98%, Shanghai yuanye Bio-Technology Co., Ltd, Shanghai, China) treatment; or 2 mg/kg of MTX treatment groups. Treatment was started on D28 with Ziyu I once daily and MTX once every 3 days for 4 weeks, with global assessments measured every 7 days before booster immunization and every 3 days after the onset of joint inflammation. The body weight gain (g) of each mouse was calculated by subtracting the body weight of each mouse on day 0. The arthritis severity of each paw was evaluated by using a macroscopic scoring system ranging from 0 to 4 (0, paws with no swelling or focal redness; 1, mild but definite redness and swelling of the ankle or wrist or apparent redness and swelling limited to individual digits, regardless of the number of affected digits; 2, moderate redness and swelling of the ankle or wrist; 3, severe redness and swelling of the entire paw, including digits; and 4, maximally inflamed limbs with the involvement of multiple joints). The cumulative score for all four paws of each mouse was used as the polyarthritis index and had a maximum value of 16 [13].

2.2. Histopathological examination of the spleen and joints

The left rear ankle joint and spleen were collected after treatment. Thymus was weighted to calculate the thymus index by comparing the thymus weight (g) to body weight (g). All mice were sacrificed on day 55. The fur and muscle were removed from ankle joint before fixation. The knee joints were collected from indicated mice and fixed in formalin for 24 h, then were subjected to decalcification in 10% EDTA. The joints and spleens were embedded into paraffin blocks and 4 μm sections were prepared for H&E staining. The slides were scanned in a 3D HISTECH panoramic scanner (3DHISTECH Ltd. Budapest, Hungary) and analyzed using included software caseviewer. The histopathological evaluation indexes and grades of joints and spleen of mice were based on previous reports. The severity of joint destruction was classifed from grade 0 to grade 4 for intensity of the lining layer hyperplasia, mononuclear cell infltration, and pannus formation. Five parameters were applied for the pathological evaluation of the spleen: the amount of red pulp, the total number of germinal centres (GCs), cellularity of the periarteriolar lymphoid sheath (PALS), lymphoid follicles, and marginal zone. The infammation was ranked on a numerical scale from 0–4 (severe change) [14].

2.3. Serum cytokine detection with ELISA

After the mice were anesthetized, peripheral blood was collected for coagulation at 37°C for 2 hours and centrifuged at 2500 RPM for 30 minutes. The supernatant was retained, and the cytokines (including IL-17 and TGF-β) were detected using Elisa kits [15]. Mouse Interleukin-17 (IL-17) ELISA Kit (Catalog #: ml037866-J) and Mouse TGF-β ELISA Kit (Catalog #: ml057830-J) were products from Shanghai Enzyme-linked Biotechnology Co., Ltd. Standard curve was used to determine the amount of TGF-β or IL-17 in unknown samples and the absorbance were recorded at 450 nm using a BioTek Elx×808 microplate reader (Lonza Group, Ltd. Basel, Switzerland).

2.4. Viability of T lymphocytes

The vitality of T lymphocytes was determined by Cell Counting Kit-8 (CCK-8) assay as previously described [14]. After treatment, T cells of thymus were prepared from the thymus of mice. 1×10^6 splenic cells were seeded evenly into each well of a 96-well plate and stimulated with Concanavalin A (ConA) (Catalog #: FMS-FZ203, FcMACS, Nanjing, China) at final concentration of 5mg/L in a 5% CO2 cell incubator for 16 hours. Two hours before the termination, 10 μl of CCK-8 solution (Catalog #: E-CK-A361, Elabscience Biotechnology, Wuhan, China) was added into each well and the cells were continued with the culture. The absorbance at 450 nm was measured on a BioTek Elx×808 microplate reader (Lonza Group, Ltd. Basel, Switzerland).

2.5. Flow cytometry

Flow cytometry was applied to detect the percentage of T lymphocyte subsets in the spleen of treated mice. After individual treatment, the mice were sacrificed through anesthetization. The spleens were ground to separate lymphocyte cells using mouse lymphocyte separation medium (Catalog #: DKW33-R0100, Dakewe Biotech Co., Ltd. Shenzhen, China). 1×10^6 cells were incubated with FITC Rat Anti-Mouse CD4 (Clone RM4-5, Catalog #: 553046, BD Biosciences, Franklin Lakes, NJ, USA) / APC Rat Anti-Mouse CD25 (Clone PC61, Catalog #: 561048, BD Biosciences, Franklin Lakes, NJ, USA) / PE Anti-Mo/Rt Foxp3 (Clone FJK-16a, Catalog #: 2344844, Elabscience Biotechnology, Wuhan, China)/ APC Rat Anti-Mouse CD3 (Catalog #: 554832, BD Biosciences, Franklin Lakes, NJ, USA) /PE Rat Anti-Mouse IL-17A (Catalog #: 553046, BD Biosciences, Franklin Lakes, NJ, USA). The samples were sufficiently mixed and incubated at 4 °C for 30 min in dark, and they were detected on Cytoflex Platform (Cytoflex S, Beckman Coulter Life Sciences, Indianapolis, IN, USA). The percentage of $CD4^+IL\text{-}17A^+$ Th17 cell and $CD4^+CD25^+Foxp3^+$ Treg cell in total T cell were analyzed by using CellQuest™ software (BD, San Diego, CA, USA).

2.6. Real-time quantitative polymerase chain reaction (RT-qPCR)

Total RNA was extracted from spleen cells using Trizol reagent following the manufacturer's protocol and then total RNA was extracted and was reversely transcribed into complementary DNA (cDNA) using cDNA synthesis kit (Catalog #: 634926, Takara Bio Inc. Otsu, Shiga, Japan) referring to the instructions. The specific primers for RORγt, Foxp3 and GAPDH are listed in Table 1. Subsequently, the cDNA template was amplified on a 7500 real-time PCR system (Applied Biosystems, Foster City, CA, USA) by applying a Fast SYBR Green Master Mix (Catalog #: 4385612, Thermo Fisher Scientific, Waltham, MA, USA). Expression changes were calculated with normalization of GAPDH values with the $2^{-\Delta\Delta Ct}$ method. The primers sequences for the RT-qPCR are listed below as Table 1.

2.7. Molecular docking analysis

There is no complete protein three-dimensional structure of Akt1 in the PDB protein database. Obtain the protein primary structure of Akt1, that is, the amino acid sequence, from the NCBI-Protein database (https://www.ncbi.nlm.nih.gov/protein/). Use the homology modeling function of Discovery Studio 2020 software to predict the three-dimensional structure of Akt1. In homology modeling, use PDB _nr95 (PDB non-redundant structure database) to find the template, select the sequence with higher sequence identity, and perform the Build Homology Models operation in the DS-Create Homology Models section to obtain the three-dimensional Akt1 structure. Docking simulation of Ziyu I with Akt1 protein was carried out with the program Discovery Studio 2020 (DS 2020, Accelrys Software Inc.). The active sites were defined and sphere of 13.7 Å according to the important amino acid residues generated around the Akt1 active site pocket by the From Receptor Cavities program in the software Define Site settings, with the active site pocket of model using LipDock, molecular dynamics (MD) simulated-annealing based algorithm module from DS 2020. The structure of protein, substrate was subjected to energy minimization using

CHARM force field as implemented in DS 2020. A full potential final minimization was then used to refine the substrate poses. Based on LipDock, energy docked conformation of the substrate was retrieved for post-docking analysis [16].

2.8. Western blotting

The expression of Akt、mTOR and phospho-Akt (p-Akt)、phospho- mTOR (p- mTOR) in splenic T cells were determined by Western blotting. Cell samples separated from individual group of mice were lysed with lysis buffer containing 10 mM of PMSF and 10 mM of phosphatase inhibitor on ice by an ultrasonic homogenizer. The soluble protein was collected by centrifugation at 12000 rpm for 30 min at 4°C and was quantified using a Pierce BCA Protein Assay Kit (Catalog #: 23227, Thermo Fisher Scientific, Waltham, MA, USA). The protein was denatured by mixing with 5× loading buffer, and then was separated by 10% SDS polyacrylamide gel electrophoresis. The PVDF membrane with transferred protein was blocked with 5% no-fat milk in 0.05% Tween 20-PBS at 37 °C for 2 hours followed by the incubation of primary antibodies against mTOR (1:200, Catalog #: 55306F, ABMART, Shanghai China), p-mTOR (1:500, Catalog #: 293133, Santa Cruz Biotechnology, CA), Akt1/2/3 mAb (1:200, Catalog #: 55561F, ABMART, Shanghai China), Phospho-Akt (Ser473) mAb (1:200, Catalog #: T56569F, ABMART, Shanghai, China), GAPDH (1:5000, Catalog #: AF0911, Affinity Biosciences, Changzhou, China) overnight at 4°C. After rinsing with 0.05% Tween 20-PBS 3 times, the membrane was incubated with corresponding secondary antibody (1:10000, Goat Anti-Rabbit IgG (H+L) HRP, Catalog #: S0001, Goat Anti-Mouse IgG (H+L) HRP, Catalog #: S0002, Affinity Biosciences, Changzhou, China) at 37°C for 2 hours. By applying the ECL Western Blotting Substrate (Catalog #: 32106, Thermo Fisher Scientific, Waltham, MA, USA), the membrane was imaged on the Image Quant LAS 500 imager (GE Healthcare Systems, Chicago, IL, USA) and the bands of the target protein were semi-quantified by GAPDH using ImageJ software (version 1.42q, NIH) [17].

2.9. Immunofluorescence

In situ expression of mTOR/p-mTOR in T cells of treated mice was detected by immunofluorescence. 4 μm thick paraffin sections of mouse spleen tissues from each group were deparaffinized, Subsequently, the tissue was infiltrated with 0.1% Triton X-100 for 30 min and sealed in PBS containing 1% BSA for one hour in the dark. Each tissue section was incubated with a mixture of rabbit mAb anti-mTOR (1:100, Catalog #: 55306F, ABMART, Shanghai China) and mouse mAb anti-p-mTOR (1:100, Catalog #: 293133, Santa Cruz Biotechnology, CA) and PE Anti-Mouse IL-17A antiboy (1:00, Catalog #: 1995433, BD Biosciences, Franklin Lakes, NJ, USA) overnight at 4°C. After rinsing with PBS for 3 times, the samples were incubated with the corresponding fluorescent secondary antibody Alexa Fluor 647 AffiniPure Goat Anti-Mouse IgG (Catalog #: 115-605-205, Jackson ImmunoResearch Inc., West Grove, PA, USA) or Alexa Fluor 594 AffiniPure Goat Anti-Rabbit IgG (Catalog #: 115-585-003, Jackson ImmunoResearch Inc., West Grove, PA, USA) for 2 hours. The nuclei were stained with DAPI for 10 min after the sections were washed 3 times with PBS, and the slides were dried and sealed with a drop of anti-fluorescence quenching mounting solution. Digital images were acquired on a Leica TCS SP8 laser scanning confocal microscope, ImageJ software (version 1.42q, NIH) was used to quantify the mean fluorescence intensity of mTOR and p-mTOR.

2.10. Statistical analysis

Data were expressed as mean ± standard deviation (SD). The analysis of variance (ANOVA) was used to determine significant differences between groups. Values of *P* less than 0.05 were considered to be significant.

3. Results

3.1 Ziyu I ameliorates the clinical pro-manifestion of CIA mice.

The body weight of CIA mice decreased significantly on day 24 compared with that after the first injection of CCII emulsion, and gradually recovered on day 34, but the body weight of CIA mice was significantly lower than that of the normal control group. 20 mg/kg Ziyu I significantly promoted body weight of CIA mice at 40 and 43 days, while MTX significantly promoted body weight of CIA mice at 46 days (Fig. 1a). After injection of the enhancer, some of the mice experienced paw swelling from day 25. All immunized mice developed joint swelling on day 28. By day 55, CIA mice still showed severe joint inflammation. From day 49, the arthritis index of CIA mice was effectively alleviated in group I of 20 mg/kg Ziyu I, while earlier pharmacological responses began to appear in MTX treatment from day 43 (Fig. 1b). Consistent with the arthritis index, mice immunized with CCII developed mild swelling beginning at day 25 and severe swelling at day 28. MTX was able to reduce the number of swollen joints in CIA mice from day 49, and 10 mg/kg or 20 mg/kg Ziyu I was able to effectively reduce the number of swollen joints in CIA mice from day 55 (Fig. 1c). On day 25, some CIA model mice developed joint swelling, nodules formed by connective tissue hyperplasia were observed in nose, tail and ear of some mice. From day 28 onwards, immunized mice scored 2-4 on the global assessment. After MTX treatment, the overall score of mice decreased from day 49, while Ziyu I administration of 10 mg/kg and 20 mg/kg improved the overall performance of CIA mice to varying degrees (Fig. 1d). The data showed that the Ziyu I treatment group was able to effectively alleviate the inflammatory response of CIA mice, although the onset time was later compared with MTX. Therefore, we speculated that Ziyu I may be a candidate natural compound for the treatment of arthritis.

3.2. Ziyu I improves the pathologic change of joints and spleen of CIA mice.

Histopathological examination was used to evaluate the therapeutic effect of Ziyu I on CIA mice. The joints of CIA mice have severe articular cartilage destruction, inflammatory synovial infiltration and synovial cell proliferation, as well as bone erosion and synovium. 10mg/kg or 20mg/kg Ziyu I or MTX treatment significantly reduced the articular cartilage damage, angiogenesis and synovial hyperplasia of CIA mice, while 5mg/kg Ziyu I had no significant

action in the improvement of joint pathology score in CIA mice (Fig. 2a, b). The normal splenic structure consists of two major functional areas: the hematopoietic red pulp and the lymphatic white pulp. The white pulp consists of the lymphatic follicles and the lymphatic sheath around the arterioles. In CIA mice, the number of germinal centers and cell density around the lymphatic sheaths were notably increased and the lymphoid follicles, marginal zone and red pulp had substantial cell proliferation. It is worth noting that 5 mg/kg Ziyu I treatment successfully reduced lymphoid folicles in the spleen of CIA mice. 10mg/kg or 20mg/kg Ziyu I, or MTX treatment significantly reduced the frequency of GC, cell density around the lymphatic sheath, lymphoid follicle size and margins district area and red pulp congestion in varying degrees (Fig. 2c, d). According to the overall performance, Ziyu I treatment significantly inhibited the pathological changes of inflamed joints, which was in line with the exterior anti-arthritis effect of Ziyu I treatment. The data also showed that Ziyu I was able to significantly improve the spleen pathology of CIA mice.

3.3. Ziyu I restores the Th17/Treg balance of CIA mice.

Compared with normal mice, CIA mice had an increased thymus index. 20mg/kg Ziyu I tended to decrease thymus index (Fig 3a). Thymus weight and thymus index have the same trend. (Fig 3b)Splenic lymphocytes were isolated from each group of mice, and the activity of T cells stimulated by ConA was detected by CCK-8 method. T cell activity in CIA mice was much greater than that of normal splenic T cells, this increase was greatly inhibited by 20 mg/kg Ziyu I or MTX treatment, suggesting that Ziyu I had a dominant role in preventing T cell overreaction in arthritic mice (Fig. 3c). CIA mice had a significantly increase in the total number of $CD3^+CD4^+$ helper T (Th) cells compared with the normal group, while the total Th cells in 20mg/kg Ziyu I treated mice were decreased with significant degrees (Fig. 3d, e). In the present study, $CD4^+CD25^+Foxp3^+$ cells were labelled to analyze the proportions of Treg cells in the spleen cell. The results showed that the proportion of Treg cells ($CD4^+CD25^+Foxp3^+$) in the spleen T cells of CIA mice treated with Ziyu I was significantly increased, which was statistically significant. 20 mg/kg Ziyu I or MTX significantly increased the proportion of Treg cells (Fig. 3f, g). Th17 cells played an important pathogenic role in autoimmune disease and mediate autoimmune responses local inflammation and tissue destruction. Flow cytometry was used to detect the percentage of Th17 in each group. The results showed that Th17 cells in CIA spleen increased significantly, which was statistically significant. 10mg/kg Ziyu I, 20 mg/kg Ziyu I or MTX could significantly inhibit the proportion of Th17 cells (Fig. 3h, i). Ziyu I was able to improve the balance of Th17/Treg to varying degrees (Fig. 3j). These data further confirmed that Ziyu I predominantly restored the homeostasis of humoral immunity in CIA mice, and Ziyu I was able to improve the Th17/Treg imbalance by increasing the percentages of Treg cells and reducing the percentages of Th17 cells.

3.4. Ziyu I decreases serum levels of pro-inflammatory cytokine and the gene expression of RORγt.

On day 55, After the mice were anesthetized, blood was taken from the eyeballs, and the serum was collected by centrifugation after standing on ice for 1 hour. The levels of TGF-β and IL-17 in the serum were detected by ELISA. TGF-β is a pleiotropic cytokine that has important regulatory effects on cell growth, differentiation and immune function, and can inhibit the proliferation of immunocompetent cells. Compared with normal mice, the level of IL-17 was significantly increased and the level of TGF-β was significantly decreased in CIA mice (Fig. 4a-c). Spleen lymphocytes of each group of mice werek isolated and treated by Ziyu I (10^{-5}mol/l) for 48h *in vitro*. The mRNA expression levels of RORγt and Foxp3 in lymphocytes were detected by RT-qPCR. The results showed that the expression level of Foxp3 in the treatment group was significantly higher than that of the CIA model group, and the expression level of RORγt was significantly lower than that of the CIA model group, suggesting that Ziyu I was able to increase Foxp3 and decrease RORγt mRNA expression level (Fig. 4d, e). These data further confirmed that Ziyu I was able to reduce the proportion of pro-inflammatory cells in CIA mice and improve joint symptoms.

3.5. Ziyu I may interact with Akt1.

The above data indicated that Ziyu I was able to inhibit the differentiation of Th17, and we know many signaling pathways may be involved in Th17 differentiation, such as Notch signaling pathway, TLR7 signaling or PI3K/mTOR signaling [18-20]. Which signaling would be the target of Ziyu I is not clear at present. Subsequently, molecular docking analysis was performed to screen the potential target of Ziyu I, which molecular weight is 766.95 with a formula as $C_{41}H_{66}O_{13}$ (Fig. 5a)**.** As a result, Akt1 showed a direct interaction with Ziyu I. The amino acid residues of Akt1 were found from NCBI protein, and the 3d protein structure of Akt was established by using the homology modeling function of DS software. The interaction between Akt1 and Ziyu I was predicted by molecular docking technology. As analyzed, Ziyu I could be directly correlated with Akt1 through van der Waals forces, hydrogen bands and non-covalent interactions (Fig. 5b) and Table 2. Three-dimensional diagram of the docking results of Ziyu I and Akt1 was also presented in Fig. 5c. The data indicates that Ziyu I may affect the differentiation of Th17 cells through regulating Akt1 activity and downstream mTOR signaling. However, this prediction needs to be verified in the fowling experiments.

3.6. Ziyu I reduces the activation of mTOR in T cells of CIA mice.

To test this hypothesis, we measured the activation of mTOR in T cells from treated mice. The expression of Akt, p-Akt, mTOR, and p-mTOR was analyzed by Western blotting. Compared with normal mice, the expression of p-mTOR and p-Akt in T cells from CIA mice was significantly increased. However, the activation of mTOR or Akt in splenic T cells of CIA mice was significantly reduced by 10mg/kg of Ziyu I treatment (Fig. 6a-e). We further detected the in-situ expression of both p-mTOR and mTOR in IL-17A positive in cells of spleen from each treated group by immunofluorescence. The results showed that 10mg/kg, 20mg/kg Ziyu I or MTX therapy significantly reduced the phosphorylation rate of mTOR. Moreover, the fluorescence intensity of p-mTOR and IL-17A was significantly positively correlated (Fig. 6f-h). In summary, the therapeutic effect of Ziyu I on experimental arthritis may be exerted by inhibiting the activity of Akt-mTOR signaling, reducing the differentiation of Th17, and thereby rescuing the balance of Th17/Treg.

4. Discussion

In this study, we have revealed that Ziyu I is able to effectively reduce clinical parameters, joint swelling, circulating pro-inflammatory cytokines, and improve joint and spleen pathological scores in CIA mice. MTX is currently the first-line drug for the treatment of RA, so in this work, MTX was set as the positive control drug. Although as shown by the data, Ziyu I has a relative low efficacy than MTX in treating CIA mice, the global assessment and pathological examinations definitely confirms that Ziyu I has a specific anti-arthritis property. The mild action of Ziyu I in CIA treatment may due to its low bioavailability because of the high fat solubility [21]. Therefore, the bioavailability of Ziyu I can be increased by changing its structure or formulating targeted drugs to specific tissue sites.

In the present study, we measured T cell subsets in Ziyu I- or vehicle-treated CIA mice to explore the potential pharmacological mechanism of Ziyu I in CIA treatment. The proportion of Th17 cells in spleen T lymphocytes of CIA mice was significantly higher than that of WT mice. On the contrary, compared with normal mice, the pool of splenic Treg cells in CIA mice was slightly reduced, leading to an imbalance of Th17/Treg, which has been accepted as one of the important pathogenesis of RA [22, 23]. Compared with CIA mice treated by vehicle, Ziyu I administration effectively reduces thymus index, T cell viability, plasma IL-17 concentration, and most importantly, the frequency of Th17 cell subset. The data suggests that the balance of Th17/Treg may be a vital target of Ziyu I in alleviating experimental arthritis.

Th17 and Treg differentiation are controlled by various signals individually [18, 19], however, Akt-mTOR signaling pathway has been reported to modulate the metabolic profile of T cells thus has a dual effect on both Th17 and Treg formation. Studies have found that mTOR is a key regulator of T cell glycolysis and metabolism, and its loss leads to the reduction of Th17 development but promotes the differentiation of Treg cells [24, 25]. Molecular simulation docking assay reveals a direct interaction of Ziyu I with Akt1 by hydrogen bonds, van der Waals forces, and non-covalent bonds, and furthermore, our data also displays that Ziyu I substantially reduces the elevated activation of Akt1 and mTOR in T cells from CIA mice with no influence on the expression level of both proteins. How does Ziyu I inhibit the activation of Akt remains to be addressed.

The main active metabolite of Ziyu I in the body is Ziyu II, which has also been observed to induce cell autophagy through inhibiting Akt/mTOR pathway [21, 26]. Ziyu I and Ziyu II have similar structures and share the same parent nucleus [21]. As shown in the molecular docking data, the interacting sites of Ziyu I to Akt1 primarily locate in the parent nucleus, proving that this structure is a promising candidate for Akt1 inhibitor development.

5. Conclusion

In summary, Ziyu I inhibits the Akt/mTOR signaling pathway in the pathological process of CIA to prevent Th17 cell differentiation and thus to restore Th17/Treg imbalance and finally alleviate inflammatory arthritic response. The results suggest that Ziyu I may be an active ingredient of Chinese herb medicine with anti-rheumatism properties, and this study will provide a new idea for the development of Ziyu I as a promising prodrug for RA treatment.

Declarations

Author Contributions

M. W carried out the experiments, data analysis, and preliminary manuscript. H.S. conduct the experiments. T.S. carried out molecular docking experiment. P.G., Y.T., Z.Z., and C.J. helped to perform the experiments. W.W. provided technical assistance and experiment platform. Q.W. designed the study, evaluated the data, and modified the manuscript for publication. All authors have read and approved the manuscript.

Declaration of Interest

The authors declare that they have no known competing financial interests or personal relationships that could have appeared to influence the work reported in this paper.

Acknowledgements

This work was financially supported by the National Natural Science Foundation of China (81973314, 81202541, and 81973332), the Anhui Provincial Natural Science Foundation for Distinguished Young Scholars (1808085J28), Collaborative Innovation Project of Key Scientific Research Platform in Anhui Universities (GXXT-2020-066), Program for Upgrading Scientific Research Level of Anhui Medical University (2019xkjT008), and Academic Funding for Top-notch Talents in University Disciplines (Majors) of Anhui Province (gxbjZD2021047).

References

1. Zhou W J, Wang DD, Tao J, Tai Y, Zhou ZW, Wang Z, et al. Deficiency of β-arrestin2 exacerbates inflammatory arthritis by facilitating plasma cell formation. Acta pharmacologica Sinica 2021;42(5): 755–766.
2. Han L, Zhang X Z, Wang C, Tang X Y, Zhu Y, Cai X Y, et al. IgD-Fc-Ig fusion protein, a new biological agent, inhibits T cell function in CIA rats by inhibiting IgD-IgDR-Lck-NF-κB signaling pathways. Acta pharmacologica Sinica 2020;41(6): 800–812.
3. Boissier MC, Assier E, Falgarone G, Bessis N. Shifting the imbalance from Th1/Th2 to Th17/treg: the changing rheumatoid arthritis paradigm. Joint Bone Spine. 2008;75(4): 373-5.

4. Zhang M, Zhong J, Xiong Y, Song X, Li C, He Z. Development of Broad-Spectrum Antiviral Agents-Inspiration from Immunomodulatory Natural Products. Viruses. 2021;13(7):1257.
5. Tong L, Nanjundaiah SM, Venkatesha SH, Astry B, Yu H, Moudgil KD. Pristimerin, a naturally occurring triterpenoid, protects against autoimmune arthritis by modulating the cellular and soluble immune mediators of inflammation and tissue damage. Clin Immunol. 2014;155(2):220-30.
6. Lachowicz S, Oszmiański J, Rapak A, Ochmian I. Profile and Content of Phenolic Compounds in Leaves, Flowers, Roots, and Stalks of Sanguisorba officinalis L. Determined with the LC-DAD-ESI-QTOF-MS/MS Analysis and Their In Vitro Antioxidant, Antidiabetic, Antiproliferative Potency. Pharmaceuticals (Basel). 2020;13(8):191.
7. Yu T, Lee YJ, Yang HM, Han S, Kim JH, Lee Y, et al. Inhibitory effect of Sanguisorba officinalis ethanol extract on NO and PGE (2) production is mediated by suppression of NF-kappaB and AP-1 activation signaling cascade. J Ethnopharmacol. 2011;134(1) :11-7.
8. Seo CS, Jeong SJ, Yoo SR, Lee NR, Shin HK. Quantitative Analysis and In vitro Anti-inflammatory Effects of Gallic Acid, Ellagic Acid, and Quercetin from Radix Sanguisorbae. Pharmacogn Mag. 2016;12(46) :104-8.
9. Yang JH, Hwang YH, Gu MJ, Cho WK, Ma JY. Ethanol extracts of Sanguisorba officinalis L. suppress TNF-alpha/IFN-gamma-induced pro-inflammatory chemokine production in HaCaT cells. Phytomedicine. 2015;22(14) :1262-8.
10. Elekofehinti OO. Saponins: Anti-diabetic principles from medicinal plants - A review. Pathophysiology. 2015;22(2) :95-103.
11. Sun A, Xu X, Lin J, Cui X, Xu R. Neuroprotection by saponins. Phytother Res. 2015;29(2) :187-200.
12. Wang R, Zhang M, Hu S, Liu K, Tai Y, Tao J, et al. Ginsenoside metabolite compound-K regulates macrophage function through inhibition of beta-arrestin2. Biomed Pharmacother. 2019;115: 108909.
13. Huang B, Wang QT, Song SS, Wu YJ, Ma YK, Zhang LL, et al. Combined use of etanercept and MTX restores CD4⁺/CD8⁺ ratio and Tregs in spleen and thymus in collagen-induced arthritis. Inflamm Res. 2012;61(11):1229-39.
14. Zhang M, Hu S, Tao J, Zhou W, Wang R, Tai Y, et al. Ginsenoside compound-K inhibits the activity of B cells through inducing IgD-B cell receptor endocytosis in mice with collagen-induced arthritis. Inflammopharmacology. 2019;27(4) :845-56.
15. Wang Y, Chen J, Luo X, Zhang Y, Si M, Wu H, et al. Ginsenoside metabolite compound K exerts joint-protective effect by interfering with cnidocyte function mediated by TNF-alpha and Tumor necrosis factor receptor type 2. Eur J Pharmacol. 2016;771: 48-55.
16. Han C, Li Y, Zhang Y, Wang Y, Cui D, Luo T, et al. Targeted inhibition of GRK2 kinase domain by CP-25 to reverse fibroblast-like synoviocytes dysfunction and improve collagen-induced arthritis in rats. Acta Pharm Sin B. 2021;11(7) :1835-1852.
17. Yang X, Zhao Y, Jia X, Wang C, Wu Y, Zhang L, et al. CP-25 combined with MTX/ LEF ameliorates the progression of adjuvant-induced arthritis by the inhibition on GRK2 translocation. Biomed Pharmacother. 2019;110:834-43.
18. Keerthivasan S, Suleiman R, Lawlor R, Roderick J, Bates T, Minter L, et al. Notch signaling regulates mouse and human Th17 differentiation. J Immunol. 2011;187(2): 692-701.
19. Ye J, Wang Y, Liu X, Li L, Opejin A, Hsueh E C, et al. (2017) TLR7 Signaling Regulates Th17 Cells and Autoimmunity: Novel Potential for Autoimmune Therapy. Journal of immunology (Baltimore, Md.: 1950), 199(3): 941–954.
20. Essig K, Hu D, Guimaraes J C, Alterauge D, Edelmann S, Raj T, et al. Roquin Suppresses the PI3K-mTOR Signaling Pathway to Inhibit T Helper Cell Differentiation and Conversion of Treg to Tfr Cells. Immunity. 2017;47(6): 1067–1082.e12.
21. Li ZF, Zhou MY, Tan T, Zhong CC, Wang Q, Pan LL, et al. A Sample and Sensitive HPLC-MS/MS Method for Simultaneous Determination of Ziyuglycoside I and Its Metabolite Ziyuglycoside II in Rat Pharmacokinetics. Molecules. 2018;23(3):543.
22. Toh ML, Miossec P. The role of T cells in rheumatoid arthritis: new subsets and new targets. Curr Opin Rheumatol. 2007;19(3) :284-8.
23. Fox DA. Citrullination: A Specific Target for the Autoimmune Response in Rheumatoid Arthritis. J Immunol. 2015;195(1): 5-7.
24. Shi LZ, Wang R, Huang G, Vogel P, Neale G, Green DR, et al. HIF1alpha-dependent glycolytic pathway orchestrates a metabolic checkpoint for the differentiation of TH17 and Treg cells. J Exp Med. 2011;208(7) :1367-76.
25. Nagai S, Kurebayashi Y, Koyasu S. Role of PI3K/Akt and mTOR complexes in Th17 cell differentiation. Ann N Y Acad Sci. 2013;1280: 30-4.
26. Bai C, Zhang Z, Zhou L, Zhang HY, Chen Y, Tang Y. Repurposing Ziyuglycoside II Against Colorectal Cancer via Orchestrating Apoptosis and Autophagy. Front Pharmacol.2020;11: 576547.

Tables

Table1. Primers for Real -Time RT-qPCR.

Genes	Forward sequence	Reverse sequence
RORγt	5'-CCGCTGAGAGGGCTTCAC-3'	5'-TGCAGGAGTAGGCCACATTACA-3'
Foxp3	5'-ATGTTCGCCTACTTCAGAA-3'	5'-TCATCTACGGTCCACACT-3'
gapdh	5'-AAATGGTGAAGGTCGGTGTGAAC-3'	5'-CGACATACTCAGCACCAGCACACT-3'

Table2. Molecular docking results of Ziyu I and Akt1.

Name	Visible	Color	Parent	Distance	Category	Types	From	From Chemistry	To	To Chemistry	An XD
:GLY311:N - Molecule:O39	Yes	0 255 0	Ligand Non-bond Monitor	3.16295	Hydrogen Bond	Conventional Hydrogen Bond	:GLY311:N	H-Donor	Molecule:O39	H-Acceptor	34.
Molecule:O8 - :GLU198:OE1	Yes	0 255 0	Ligand Non-bond Monitor	2.39578	Hydrogen Bond	Conventional Hydrogen Bond	Molecule:O8	H-Donor	:GLU198:OE1	H-Acceptor	38.
Molecule:O39 - :GLY311:O	Yes	0 255 0	Ligand Non-bond Monitor	2.76935	Hydrogen Bond	Conventional Hydrogen Bond	Molecule:O39	H-Donor	:GLY311:O	H-Acceptor	58.
Molecule:O53 - :GLU191:OE2	Yes	0 255 0	Ligand Non-bond Monitor	3.12446	Hydrogen Bond	Conventional Hydrogen Bond	Molecule:O53	H-Donor	:GLU191:OE2	H-Acceptor	10
Molecule:O54 - :GLU191:O	Yes	0 255 0	Ligand Non-bond Monitor	2.94754	Hydrogen Bond	Conventional Hydrogen Bond	Molecule:O54	H-Donor	:GLU191:O	H-Acceptor	11.
Molecule:O54 - :GLU191:OE1	Yes	0 255 0	Ligand Non-bond Monitor	3.18369	Hydrogen Bond	Conventional Hydrogen Bond	Molecule:O54	H-Donor	:GLU191:OE1	H-Acceptor	71.
:LYS189:CE - Molecule:O51	Yes	220 255 220	Ligand Non-bond Monitor	3.69103	Hydrogen Bond	Carbon Hydrogen Bond	:LYS189:CE	H-Donor	Molecule:O51	H-Acceptor	55.
:GLY294:CA - Molecule:O3	Yes	220 255 220	Ligand Non-bond Monitor	3.30633	Hydrogen Bond	Carbon Hydrogen Bond	:GLY294:CA	H-Donor	Molecule:O3	H-Acceptor	39.
Molecule:C2 - :GLU191:OE1	Yes	220 255 220	Ligand Non-bond Monitor	3.43971	Hydrogen Bond	Carbon Hydrogen Bond	Molecule:C2	H-Donor	:GLU191:OE1	H-Acceptor	46.
:LEU295 - Molecule	Yes	255 200 255	Ligand Non-bond Monitor	4.39062	Hydrophobic	Alkyl	:LEU295	Alkyl	Molecule	Alkyl	
:LEU295 - Molecule	Yes	255 200 255	Ligand Non-bond Monitor	4.31109	Hydrophobic	Alkyl	:LEU295	Alkyl	Molecule	Alkyl	
Molecule:C38 - :CYS310	Yes	255 200 255	Ligand Non-bond Monitor	4.85729	Hydrophobic	Alkyl	Molecule:C38	Alkyl	:CYS310	Alkyl	
:PHE309 - Molecule:C37	Yes	255 200 255	Ligand Non-bond Monitor	5.12019	Hydrophobic	Pi-Alkyl	:PHE309	Pi-Orbitals	Molecule:C37	Alkyl	

Figures

Fig1.

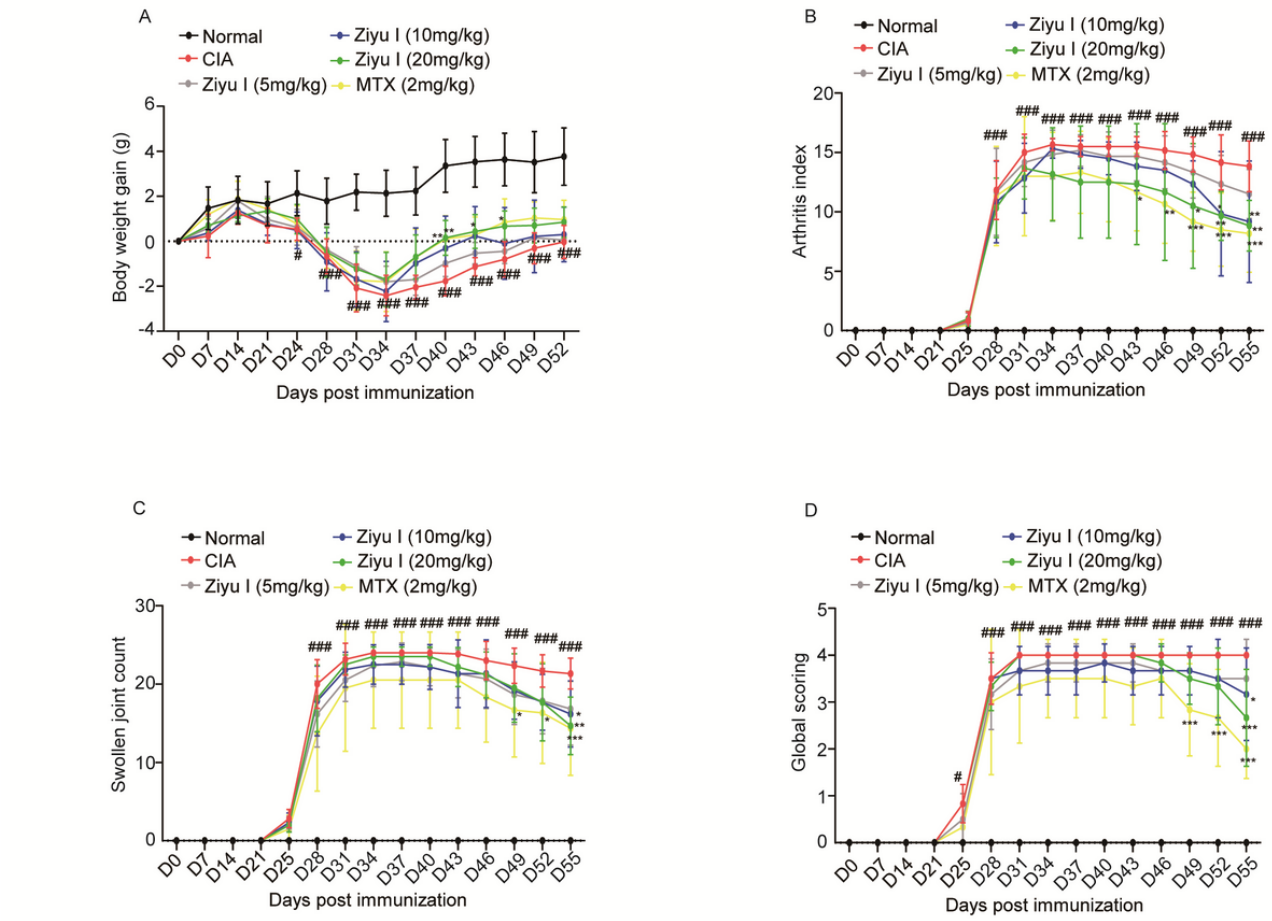

Figure 1

Ziyu I treatment effectively improved the manifestations of mice with CIA. (a) Body weight gain (g). (b) Arthritis index. (c) Swollen joint count. (d) Global scoring. The data were expressed as mean ± SD, n=5~6. #P < 0.05, ##P < 0.01, ###P < 0.001 vs. Normal. *P < 0.05, **P < 0.01, ***P < 0.001 vs. CIA.

Fig2

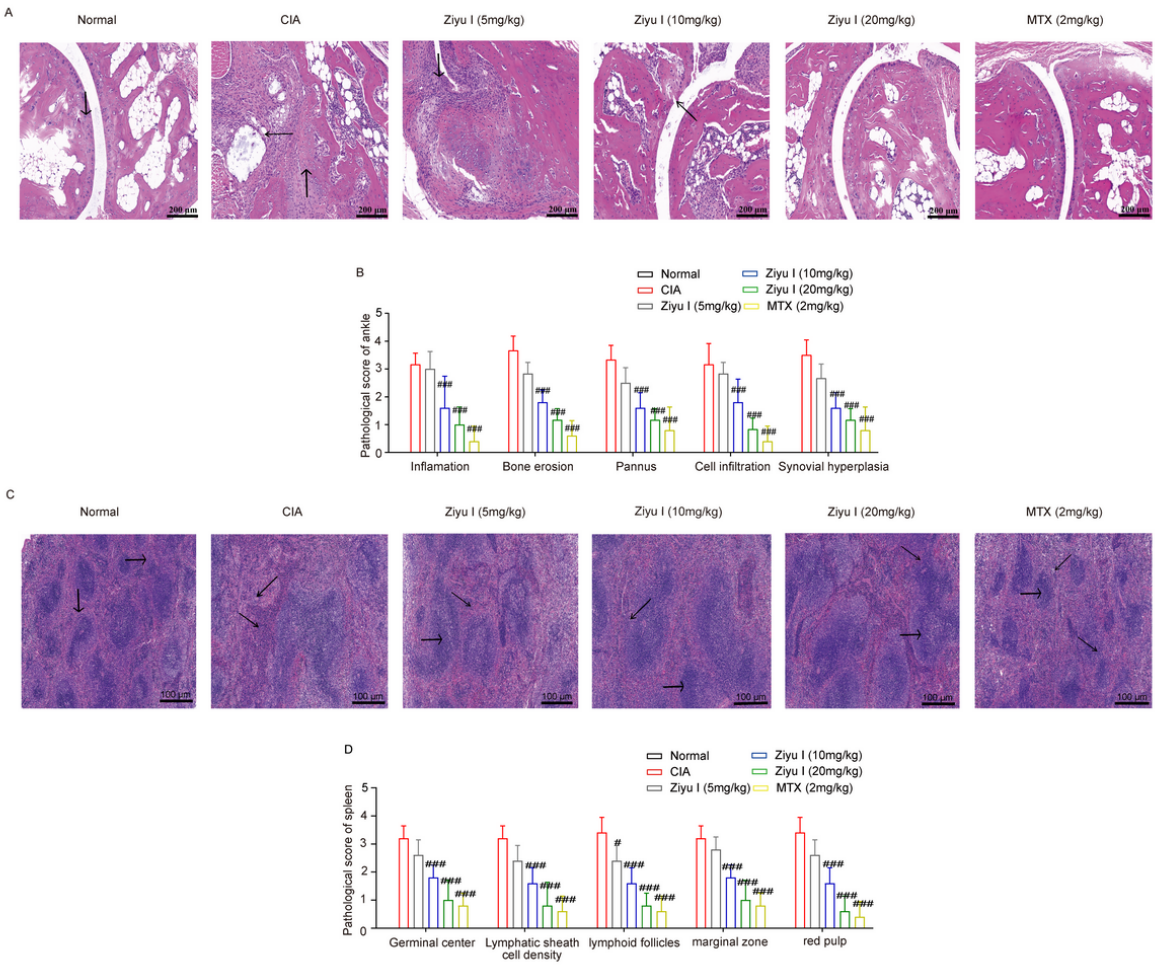

Figure 2

Effects of different doses of Ziyu I on the histopathology of ankle and spleen of CIA mice. (a) Representative pathological images of ankle. In normal mice,→shows red pulp and↓shows white pulp. In CIA mice,→shows germinal centers,↓shows lymphoid follicular hyperplasia, ↙shows periarteriolar lymphoid sheaths, and ↘ shows red medullary congestion. (b) Analysis of ankle pathological scores. (c) Representative pathological images of spleen. In normal mice,↓shows the synovial membrane. In CIA mice,↑shows synovial hyperplasia, ↓shows inflammatory cell infiltration, ← shows vascular pannus, and ↖ shows cartilage damage. (d) Analysis of spleen pathological scores. The data were expressed as mean ± SD, n=5. #P < 0.05, ##P < 0.01, ###P < 0.001 vs. CIA.

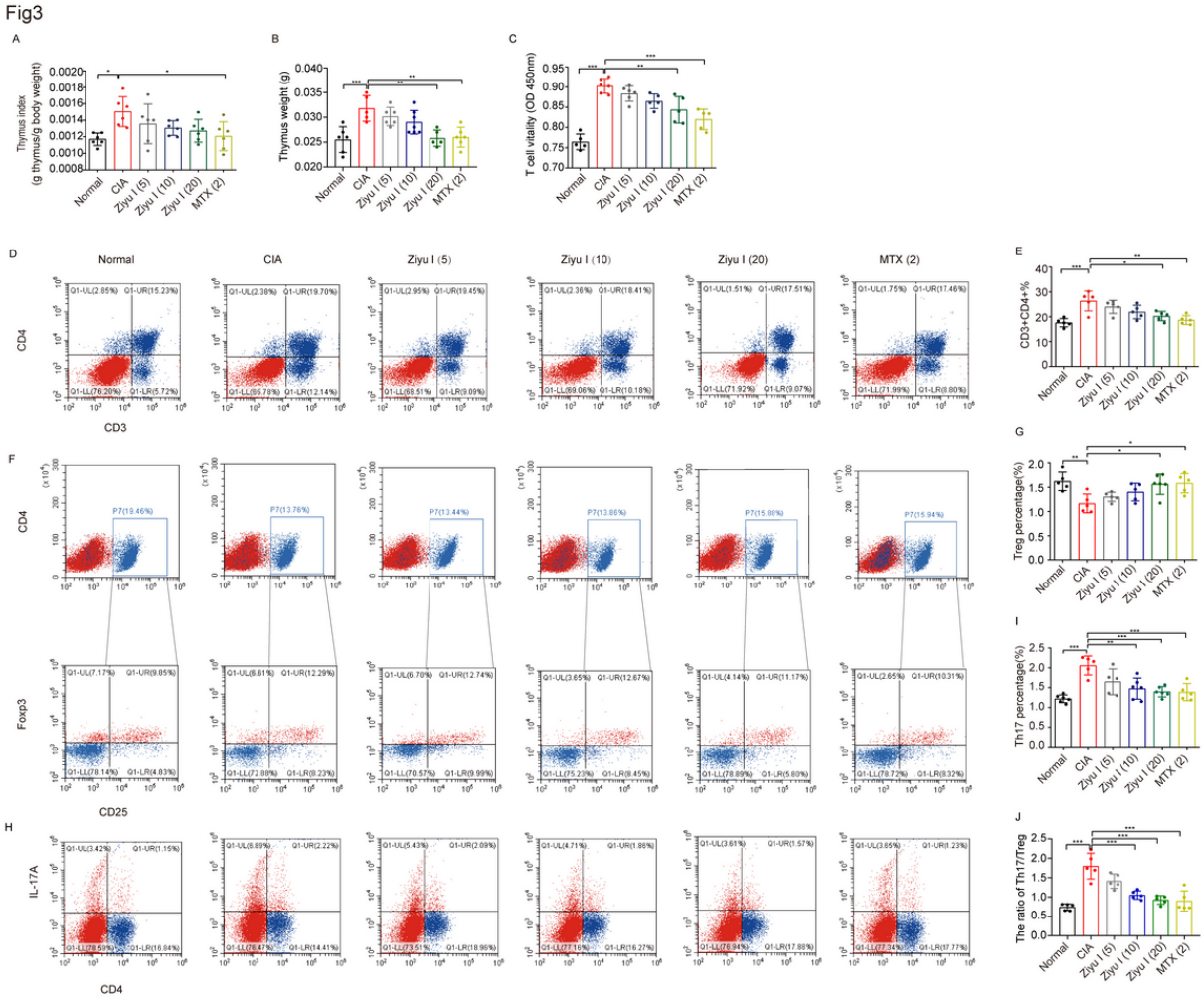

Figure 3

Ziyu I treatment can reduce the proportion of Th17 cells in CIA mice. (a) The thymus index (g thymus/g body weight) of treated CIA mice was calculated. (b)Thymus weight (g). (c) T cells vitality was tested by CCK-8. (d) Representative flow cytometry scatter plot of $CD3^+CD4^+$ Th cells. (e) The percentage of Th cells were analyzed. (f) Representative flow cytometry scatter plot of $CD4^+CD25^+Foxp3^+$ Treg cells. (g) The percentage of Treg cells were analyzed. (h) Representative flow cytometry scatter plot of Th17 cells. (i) The percentage of Th17 cells were analyzed. (j) The ratio of Th17/Treg cells were analyzed. *P < 0.05, **P < 0.01, ***P < 0.001 vs. CIA. (n = 5~6, mean ± SD).

Fig4

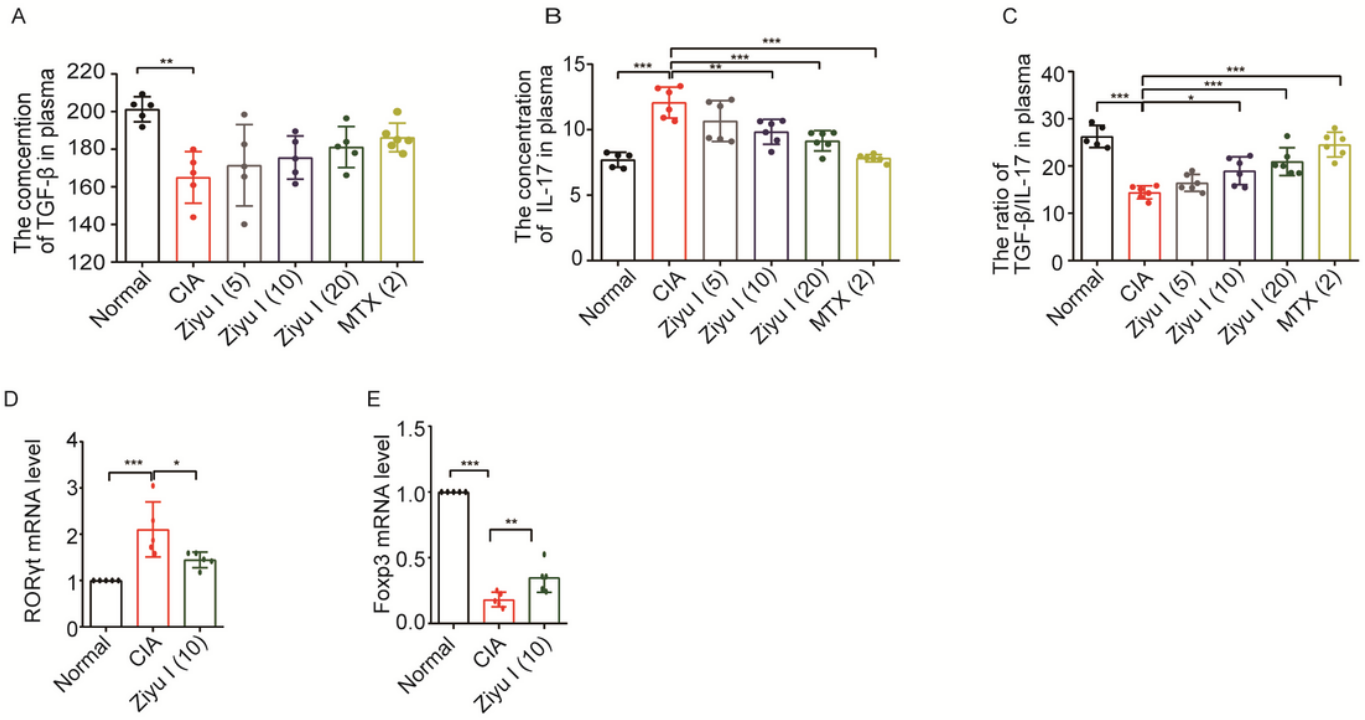

Figure 4

Effects of different doses of Ziyu I on splenic T cells of CIA mice. (a) Plasma TGF-β level (pg/ml) (b) Plasma IL-17 level (pg/ml) (c) Plasma TGF-β/IL-17 level. (d) The mRNA expression of RORγt was determined by RT-qPCR. (e) The mRNA expression of Foxp3 was determined by RT-qPCR. The concentration was calculated according to the absorbance at 450 nm. *P < 0.05, **P < 0.01, ***P < 0.001 vs. CIA. (n = 5~6, mean ± SD)

Fig5

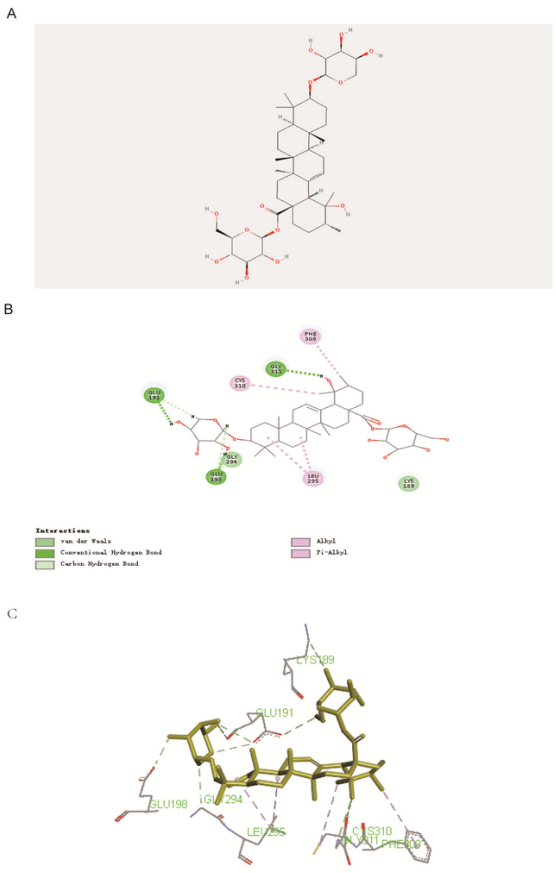

Figure 5

Based on molecular docking to find the mechanism of Ziyu I in the treatment of CIA mice. (a) Molecular structure of Ziyu I (b) A plan view of the docking results of Ziyu I and Akt1. Gray represents the ligand Ziyu I the dotted line represents the existing interaction force between the ligand and the receptor. (c) Three-dimensional diagram of the docking results of Ziyu I and Akt1. Gray represents the receptor Akt1, green represents the ligand Ziyu I, red represents the interface receptor residues. The dotted line represents the existing interaction force between the ligand and the receptor.

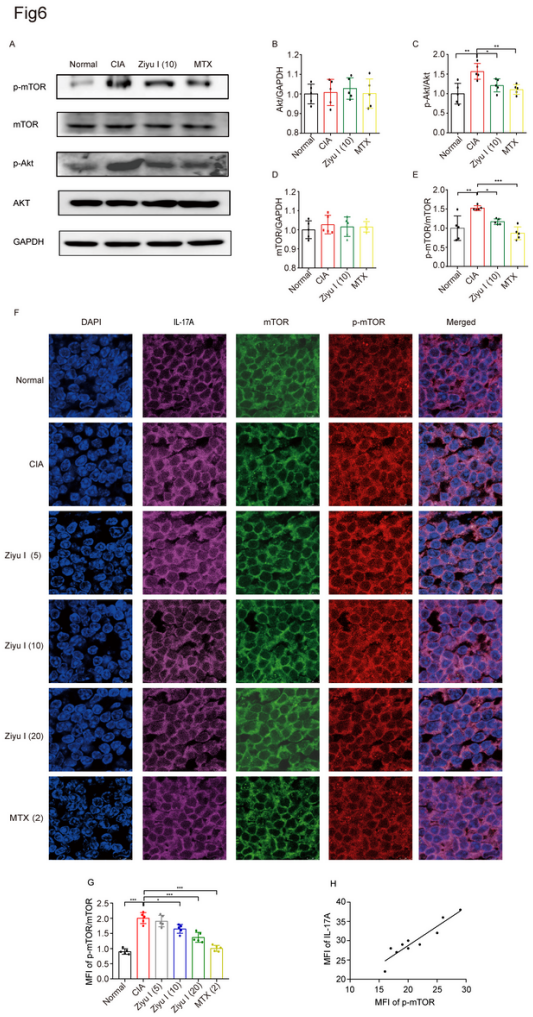

Figure 6

Ziyu I treatment reduces the activation of mTOR in T cells of CIA mouse. (a) The relative expression of Akt□mTOR and p- Akt□p-mTOR in splenic T cells from normal mouse, CIA mouse and 10 mg/kg Ziyu I treatment mouse. (b) The analysis of Akt/GAPDH expression (c) The analysis of p-Akt/Akt expression (d) The analysis of mTOR/GAPDH expression (e) The analysis of p-mTOR/mTOR expression (f) Representative immunofluorescence images of mTOR, p-mTOR and IL-17A labelling in spleen tissue of CIA mice. (g) The mean fluorescence intensity of p-mTOR/mTOR in the spleens of mice was analyzed by immunofluorescence (h) Correlation analysis between MFI of p-mTOR and MFI of IL-17A in the spleen tissue of CIA mice. The data are presented as mean ± SD, n=5. *P < 0.05, **P < 0.01, ***P < 0.001 vs. CIA.